

Journal of Materials Chemistry B

Accepted Manuscript



This is an *Accepted Manuscript*, which has been through the Royal Society of Chemistry peer review process and has been accepted for publication.

Accepted Manuscripts are published online shortly after acceptance, before technical editing, formatting and proof reading. Using this free service, authors can make their results available to the community, in citable form, before we publish the edited article. We will replace this *Accepted Manuscript* with the edited and formatted *Advance Article* as soon as it is available.

You can find more information about *Accepted Manuscripts* in the [Information for Authors](#).

Please note that technical editing may introduce minor changes to the text and/or graphics, which may alter content. The journal's standard [Terms & Conditions](#) and the [Ethical guidelines](#) still apply. In no event shall the Royal Society of Chemistry be held responsible for any errors or omissions in this *Accepted Manuscript* or any consequences arising from the use of any information it contains.

Cite this: DOI: 10.1039/c0xx00000x

www.rsc.org/xxxxxx

ARTICLE TYPE

Humic acid assisted synthesis of stable copper nanoparticles as peroxidase mimetic and their application in glucose detection

Nan Wang, Bingchen Li, Fengmin Qiao, Jianchao Sun, Hai Fan*, Shiyun Ai*

Received (in XXX, XXX) Xth XXXXXXXXXX 20XX, Accepted Xth XXXXXXXXXX 20XX

DOI: 10.1039/b000000x

In this report, stable copper nanoparticles (Cu NPs) were prepared by a facile annealing process using humic acid as the reducing and stabilizing agent. The products were characterized by X-ray powder diffraction, scanning electron microscope and Fourier transform infrared spectroscopy. The prepared Cu NPs show remarkable intrinsic peroxidase-like activity, which can fleetly catalyze the oxidation of peroxidase substrate 3, 3', 5, 5'-tetramethylbenzidine (TMB) in the presence of H₂O₂ to produce a blue color reaction. The detection limit of H₂O₂ by Cu NPs can be as low as 1.32×10^{-7} M. More importantly, the prepared Cu NPs shows excellent stability, which can hardly be oxidized even after 6 months. Based on the above mechanism, a simple, rapid and selective colorimetric method for the glucose detection was developed, and the detection limit of the glucose was 6.86×10^{-7} M. This work provides a novel method for the preparation of stable Cu NPs, which may have wide applications on the detection of glucose in human body and pear juice.

1. Introduction

Glucose is indispensable in life cycles and involved in the reaction of the organism's metabolism. Generally, alternations in glucose level directly link to a number of diseases associated with the eyes, kidneys, heart, blood vessels, nerve of chronic damage and dysfunction^{1,2}. Therefore, detecting the concentration change of glucose in real time is obligatory. At present, the most common method for detecting glucose is by the detection of H₂O₂ produced during glucose oxidase catalyzing glucose oxidation, while peroxidase can catalyze the oxidation of peroxidase substrate TMB in the presence of H₂O₂ to produce a color reaction under very mild and favorable biological conditions^{3,4}. However, the applications of these enzymes are limited owing to their intrinsic properties (such as easy denaturing under extreme pH and high temperatures), rigorous storage requirements and high cost⁵. Therefore, artificial enzymes have aroused extensive attention because of their stability, highly catalytic activity and wide range of reaction conditions.

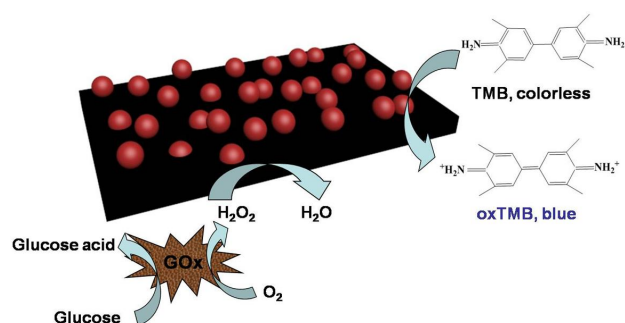
Recently, nanomaterials have received intense interests as enzyme mimetics due to their unique size, shape, composition, and structure-dependent properties. Gao et al. reported Fe₃O₄ nanoparticles have the peroxidase-like activity which paved the way for nanoparticles as enzyme mimics⁶. From then on, a lot of literatures reported numerous nanomaterials possessing peroxidase-like activity. Recently, the widespread application of noble metal nanostructures has attracted great interest⁷. Noble metal nanoparticles such as Ag nanoclusters^{8,9}, cubic Pt nanocrystals¹⁰, positively charged gold nanoparticles^{11,12}, BSA-stabilized Au^{13,14} and BSA-stabilized Pt nanoclusters¹⁵⁻¹⁷, have also been found to possess enzyme-like activities. However, high

cost of those noble metal nanoparticles largely limits their applications. More recently, bimetallic nanoparticles¹⁸⁻²⁰ and hybrids nanomaterials^{21,22} have been synthesized as the peroxidase nanomaterials, however, the synthetic method is complicated with many complex steps. In a word, to improve the catalytic efficiency and reduce the costs, a cheap, simple and one-step preparation method of metal nanoparticles with peroxidase-like activity is highly desired.

Compared with noble metal nanostructures, copper is cheaper than noble metals, which supports its wide range of applications such as catalysts²³⁻²⁵, sensors²⁶⁻²⁹ and biomedicine^{30,31}. However, the chemical synthesis of Cu nanostructures was limited due to the difficulty in reducing Cu salts to metallic Cu, and the easy oxidization of Cu nanostructures in the presence of air^{32,33}. In some synthetic processes of Cu nanocrystals, hydrazine has been proved to be an effective reducing agent³⁴⁻³⁶. However, using this method, the yield of the products was too low to be satisfied. Meanwhile, hazardous hydrazine is undesirable. In 2010, Bartosz A. Grzybowski and his co-workers reported that low-polydispersity copper nanoparticles (NPs) and nanorods (NRs) were synthesized by thermal decomposition of copper (II) acetylacetonate precursors in the presence of surfactants³⁷. However, these copper nanoparticles were stabilized with easily-broken bound alkylamine ligands. Xia and co-workers reported the synthesis of Cu nanocrystals with hexadecylamine serving as a capping agent³⁸. Therefore, it is challenging to develop a synthetic method of stable Cu NPs with peroxidase-like activity. Without protective or stabilizing agent, Cu NPs are easy to aggregate due to its high surface energy, which could cause the rapid decay of its catalytic activity and stability³⁹. Seldom reports have applied Cu NPs as peroxidase mimetics due to their low

stability property. Recently, Lianzhe Hu et al.⁴⁰ prepared Cu nanoclusters and applied them as peroxidase mimetics for detection of H₂O₂ and glucose. However, they did not investigate the structural stability of the Cu nanoclusters.

In this study, a simple method was proposed to synthesize stable Cu NPs. The stable Cu NPs were synthesized using humic acid as a reducing and stabilizing agent at 600 °C for 2 hours. Additionally, the studies on the stability of Cu nanoparticles indicated excellent stability property, which can hardly be oxidized even after 6 months. Furthermore, we discovered that the Cu NPs have wonderful intrinsic peroxidase-like activity, which can fleetly catalyze the oxidation of peroxidase substrate 3, 3', 5, 5'-tetramethylbenzidine (TMB) in the presence of H₂O₂ to produce a blue color reaction. Thus, a simple, sensitive and selective colorimetric method for glucose detection has been established (scheme 1) and used for the glucose detection in blood and pear juice samples. This work provides a stable peroxidase mimetic with low cost and high catalytic activity, which would have wide applications in medical diagnostics and biotechnology fields.



Scheme 1 Schematic of detection of glucose by using glucose oxidase and Cu NPs-catalyzed reaction.

2. Experimental

2.1 Chemical reagents and apparatus

TMB, glucose oxidase (GOx) and humic acid were purchased from Aladdin (Shanghai, China). Copper acetate, H₂O₂, glucose, fructose, lactose and maltose were purchased from Kay Tong Chemical Reagents Co., Ltd (Tianjin, China). The blood samples were provided by the University Hospital. All reagents employed were of analytical grade and used without further purification. Phosphate buffer solution (PBS, pH from 2.0 to 10.0) was used in this work and double distilled deionized water was applied throughout the experiment.

2.2 Synthesis and characterization of the Cu NPs

During the synthetic process, 5.0 g copper acetate and 2.5 g humic acid were added into a 250 mL conical flask. Then a certain amount of water was added with vigorous stirring. After the adsorption saturation, the solution was centrifuged and washed with water three times and dried at 60 °C. The dried samples were grinded on the agate mortar. Then the mixture was put into a porcelain crucible covered with a lid and heated at 3 °C/min up to 600 °C for 2 hours in the nitrogen atmosphere. The different mass ratios of copper acetate and humic acid were also operated in the same procedure.

X-ray powder diffraction (XRD, Rigaku DLMAX-2550V) was

used to characterize the phase of as-synthesized products. The morphologies of the products were characterized by field emission scanning electron microscope (FESEM, S4800). Fourier transform infrared (FTIR) spectra were performed on a Bruker-Tenson 27. Kinetic measurements and UV-Vis absorption spectra were carried out on a UV-2450 Shimadzu spectrometer (Japan). Photographs were taken using a Canon G11 digital camera. A Guohua SHA-C constant-temperature shaker (Shanghai, China) and a Jingli Ld4-2 low-speed centrifuge (Beijing, China) were used in this work.

2.3 Study on catalytic activity and the detection of glucose

Peroxidase-like activity of Cu NPs was explored in 400 μL reaction solution with 800 μM TMB as a substrate in the absence or presence of H₂O₂. Moreover, catalytic experiments were performed when the concentration of substrate TMB was constant and the concentration of Cu NPs or H₂O₂ was varied respectively. At a wavelength of 652 nm, the kinetic measurements were carried out in time course mode³⁴. And double reciprocal plots of the activity of Cu NPs were obtained with the concentration of one substrate (TMB or H₂O₂) constant and the other varied. The Lineweaver-Burk double reciprocal plot: $1/v = (K_m/V_{max})(1/[S]) + 1/V_{max}$ was used to calculate the Michaelis-Menten constant. In this equation, v is the initial velocity, V_{max} is the maximal reaction velocity, and $[S]$ is the concentration of the substrate⁴¹⁻⁴³.

Glucose detection was done in air-saturated solution as previously reported³⁴. 5 μL 40 mg/mL GOx was added to 100 μL glucose of different concentrations. Then, they were incubated at 37 °C for one hour. Firstly, 95 μL 25 mM PBS (pH 3.0) was added into the above 105 μL glucose reaction solution. Then 100 μL 8 mM TMB ethanol solutions and 100 μL Cu NPs suspension solutions were added into the above reaction solutions. After reacted for 10 min, the absorption spectra were measured.

For glucose determination in blood and pear juice, the samples were firstly treated by centrifugation at 12000 rpm for 40 min and then the supernatants were diluted with 0.5 mM buffer (pH 7.0) for the next-step measurement.

3. Results and discussion

3.1 Characterizations of Cu NPs

X-ray powder diffract meter (XRD) was conducted to investigate the crystal structures and phase purities of the as-synthesized products. In the XRD pattern (Fig. 1A), all the diffraction peaks can be indexed to that of standard pattern in the PDF card (04-0836) with a primitive hexagonal unit cell. No other characteristic peaks of impurities, such as CuO or Cu₂O, were present. Fig. 1B shows the XRD pattern of Cu NPs after exposing to air for 6 months, almost as same as that of freshly prepared Cu NPs. This demonstrates that few Cu NPs have been oxidized to CuO or other Cu based compounds even after staying in air for such a long time, indicating the excellent stability of our prepared Cu NPs. The XPS characterization of the Cu NPs was provided in Fig. S1A. The dominant Cu 2p_{3/2} peak at 932.7 eV and the small Cu 2p_{5/2} peak at 952.6 eV can be assigned to Cu (0). These peaks are in consistent with those of the Cu NPs⁴⁴, which further confirms the successfully synthesis of Cu NPs. The morphology of the Cu NPs was characterized by FESEM. The SEM images (Fig. 1C) show that the Cu NPs have an average diameter of 80-

120 nm. These nanoparticles were adhered on the surface of or well wrapped by humic acid, which can also be confirmed by the TEM image (Fig. S1B). These results clearly demonstrate that stable Cu NPs have been successfully prepared, and the high stability property of Cu NPs may be mainly due to the stabilizing and reducing properties of humic acid. In addition, Cu NPs obtained at different raw mass ratios of copper acetate and humic acid were characterized by FESEM, as shown in Fig. S2. As the ratio increased, the distribution density of Cu nanoparticles changed little, indicating that Cu²⁺ ions can be well distributed in humic acid to form uniform distributed Cu NPs. However, the size of Cu nanoparticles gradually increased. While the ratio is up to 2.5:2.5, the size of Cu nanoparticles almost kept the same.

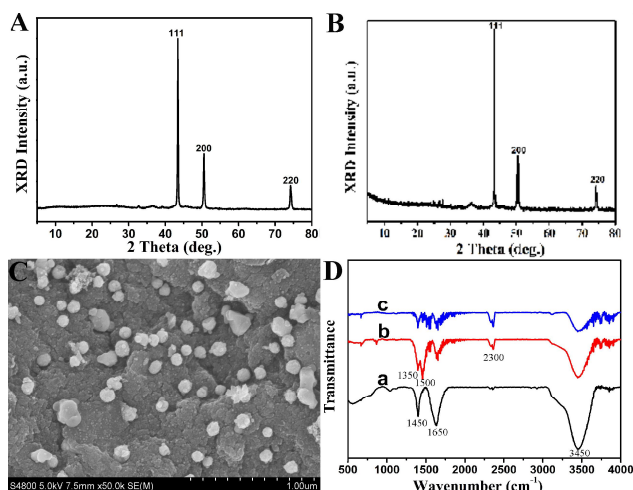


Fig. 1 XRD patterns of Cu NPs (A) freshly prepared and (B) after 6 months in air, FESEM image of the fresh Cu NPs (C), and (D) FTIR spectra of (a) humic acid, (b) humic acid calcinated at 600 °C for 2 h, (c) the co-calcinated product of humic acid and copper acetate at 600 °C for 2 h.

The FTIR spectra of three products (Fig. 1D) are employed to confirm the changes of humic acid during the synthesis of Cu NPs. The absorption band at 3450 cm⁻¹ is ascribed to the stretching of O-H and N-H, the peak at 1350 cm⁻¹ is due to the stretching vibration of C-O, the peaks at 1460 cm⁻¹ and 1650 cm⁻¹ are assigned to the vibration of C-H and C-C respectively, and the 2300 cm⁻¹ absorption peak represents the stretching of C≡N. Compared with pure humic acid (curve a in Fig. 1D), in the calcinated humic acid (curve b in Fig. 1D), the intensity of peaks at 3450 cm⁻¹ and 1500 cm⁻¹ become weakened, but at 2300 cm⁻¹, little enhancement could be observed, which indicates that C-H and O-H in the humic acid changed little. And a new peak appearing at 2300 cm⁻¹ confirms that C≡N bond was formed after the humic acid was calcinated in N₂ atmosphere. In addition, although the intensities of these characteristic peaks are decreased (curve c in Fig. 1D), the positions of these characteristic peaks are almost unchanged. Moreover, the peaks at 1650 cm⁻¹ and 3500 cm⁻¹ indicate that the carboxyl and hydroxyl are still partly remaining in humic acid, which can protect Cu NPs well. The Raman spectra demonstrate that two obvious bands at 1330 cm⁻¹ and 1600 cm⁻¹ are attributed to the carbon material⁴⁴. The Raman shift at 2800 cm⁻¹ comes from the humic acid according to the Raman spectra of humic acid. The Raman and TGA spectra (Fig. S3C and S3D) further confirm that humic acid is not completely

converted to carbon material. Therefore, in the final product, humic acid is only transformed to partially polymerized humic acid at 600 °C.

In order to further testify the stability of Cu NPs, the XRD and SEM images of the Cu NPs before and after participating in the catalytic reaction were measured as shown in Fig. 2. The XRD pattern of Cu NPs after catalytic reaction (Fig. 2A) was matched well with that of the freshly prepared Cu NPs (Fig. 1A) and that of Cu NPs after exposing to air for 6 months (Fig. 1B), indicating the stability of Cu NPs during the catalytic reaction process. Meanwhile, the FESEM image (Fig. 2B) can also confirm that the morphology of Cu NPs after catalytic reaction was almost unchanged compared with that of freshly prepared Cu NPs in Fig. 1C.

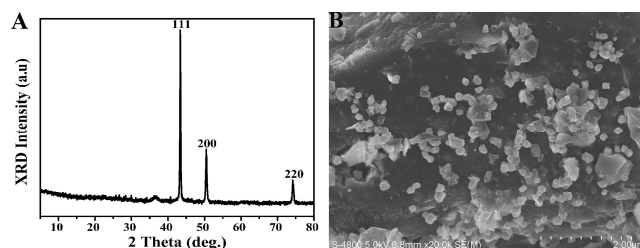


Fig. 2 XRD pattern (A) and FESEM image (B) of Cu NPs after participating in the catalyst reaction.

3.2 Peroxidase-like activity of Cu NPs and optimization of conditions

To study the peroxidase-like activity of Cu NPs, absorbance spectra were carried out in different reaction systems. As shown in Fig. 3A, the TMB + Cu NPs system shows a negligible absorbance at 652 nm. The spectrum of TMB+ H₂O₂ system without Cu NPs catalyst shows almost no difference to that of TMB + Cu NPs system. The absorbance spectra of system TMB+H₂O₂+product from the direct annealing of humic acid (namely the ratio of copper to humic acid is 0:1) in TMB oxidation by hydrogen peroxide is higher than the systems (a and c). But the absorbance at 652 nm for TMB reaction solution catalyzed by Cu NPs in the presence of H₂O₂ increased intensively. This is corresponding to the different color intensity in various systems as shown in Fig. 3B. These results clearly show that Cu NPs can well catalyze H₂O₂ oxidizing the TMB to produce a blue color reaction, indicating that our prepared Cu NPs possess excellent intrinsic peroxidase-like activity. In addition, we conducted a series of experiments by adjusting the raw mass ratio of copper acetate and humic acid, and investigated the influence on the catalytic activity of the products, as shown in Fig. S4. The catalytic activity of Cu NPs with different raw mass ratios from 1.0:2.5, 2.5:2.5, 5.0:2.5 to 7.5:2.5 was conducted. It was found that with the ratio increased from 1.0:2.5 to 2.5:2.5, the catalytic activity increased correspondingly, however, further increased, the catalytic activity kept almost the same.

Similar to peroxidase, the catalytic activity of Cu NPs is dependent on pH, temperature and other experimental conditions. Herein, the optimum pH and temperature for Cu NPs were explored to ensure that the Cu NPs could reach its highest level of activity. Phosphate buffer was selected as the reaction medium. The activity of Cu NPs was investigated with the pH of phosphate buffer varying from 2.0 to 7.0. Fig. 3C shows that the

absorbance is up to the maximum when the pH was 3.0. In Fig. 3D, as the temperature increased from 20 °C to 35 °C, the absorbance at 652 nm first increased slightly and then significantly. After 35 °C, it decreased dramatically. Therefore, pH 3.0 and 35 °C are chosen as the optimum pH and temperature in the following experiments except with special instructions or marked.

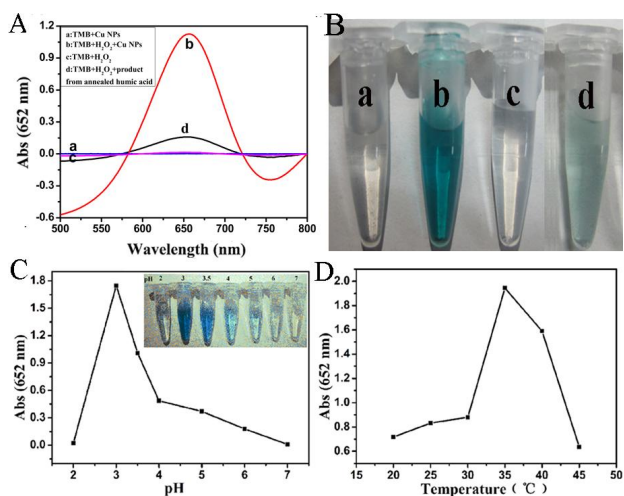


Fig. 3 (A) Absorbance spectrum of TMB (800 μM) in different reaction systems. Solutions in 100 μL 25 mM PBS (pH 3.0) incubated at the room temperature for 10 min and (B) photographs of solutions in different systems. Dependence of peroxidase-like activity of Cu NPs on (C) pH and (D) temperature. Experiments were carried out using 1 mg/mL Cu NPs in 400 μL of 100 μL 25 mM PBS with 100 μL 25 mM H₂O₂ and 100 μL 800 μM TMB as substrates. Inset: photographs of solutions in different pH values.

3.3 Michaelis constant determination

To test the catalytic activity of Cu NPs, influence of its concentration on the catalytic reaction were studied. The time-dependent absorbance at 652 nm changes when 800 μM TMB was mixed with different concentrations of Cu NPs (Fig. S5). The time-dependent absorption curves are not very smooth because the solutions may not mix uniformly before tested. However, the reaction rate is promoted with increasing sample concentration, and the concentration of 125 μg·mL⁻¹ was used in the following research due to the fine absorption curve.

Further research was performed to analyze the catalytic mechanism. Michaelis-Menten constant with H₂O₂ and TMB as substrates was measured. Kinetic data were obtained by changing one substrate concentration with the other concentration unchanged. In Fig. S6A and S6B, Michaelis-Menten curves can be given for both H₂O₂ and TMB in a range of concentrations of one substrate, and a series of the initial reaction rates were calculated. The double reciprocal plots were obtained according to the calculated series of the initial reaction rates. In Fig. S6C, every straight line was obtained by reciprocal initial velocity changing with reciprocal TMB concentration while keeping the H₂O₂ concentration constant. Three approximate parallel lines were obtained by varying concentration of H₂O₂. Similarly, reciprocal initial velocity versus reciprocal H₂O₂ concentration was collected by varying concentration of TMB as shown in Fig. S6D. The results show that the slopes of the plots are almost the same, which should be the characteristic of a ping-pong

mechanism. Moreover, Lineweaver-Burk plot was used to calculate Michaelis-Menten constant (K_m) and maximal reaction velocity (V_{max}) in this system. And the calculated values are recorded (Table S1). The peroxidase-like activity of Cu NPs with H₂O₂ and TMB as substrates was concluded according to the data in the table.

3.4 Detection of H₂O₂ and glucose using the Cu NPs

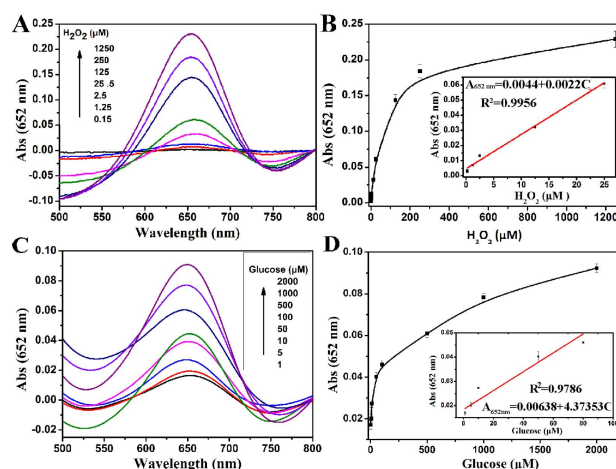


Fig. 4 (A) Absorption spectra of TMB reaction solutions catalyzed by Cu NPs in the absence or presence of different concentrations of 100 μL H₂O₂ in 100 μL 25 mM PBS (pH = 3.0) at 37 °C temperature. (B) Linear calibration plot for H₂O₂ solutions in the absence or presence of different concentrations of H₂O₂. (C) Absorbance spectra in the TMB reaction solutions catalyzed by material in the presence of different concentrations of glucose in 25 mM PBS (pH 3.0) at the room temperature. (D) A dose-response curve for glucose detection. Inset: linear calibration plot for glucose. The error bars shown are the standard errors derived from three measurements.

The excellent peroxidase-like activity of Cu NPs was testified by the above series of experiments. On this basis, the colorimetric method was developed to determinate H₂O₂ and glucose. The catalytic activity of Cu NPs is H₂O₂-concentration-dependent, and thus can be used to detect H₂O₂. Fig. 4A shows the typical H₂O₂ concentration-response curve under the optimal conditions (pH 3.0, 35 °C). In Fig. 4B, the linear calibration plot ranges from 1.5×10^{-7} to 1.25×10^{-5} M. The detection limit (S/N = 3) for H₂O₂ is 1.32×10^{-7} M under the optimal conditions. H₂O₂ is the main product of glucose oxidase oxidating glucose in the presence of O₂. A facile colorimetric approach for glucose detection can also be established according to the linear relationship between glucose and H₂O₂ as shown in scheme 1. The typical glucose concentration-response curve in Fig. 4C reveals that the glucose can be visually determined. From the linear calibration plot of Fig. 4D, the linear range of glucose detection is from 1×10^{-6} to 1×10^{-4} M with a detection limit (S/N = 3) of 6.86×10^{-7} M. The peroxidase-like activity of Cu NPs is compared with that of gold nanoparticles in Table S1. The detection limit of glucose in this assay is lower than those of previous reports based on Fe₃O₄ nanoparticles (3×10^{-5} M) or [FeIII(biuret-amide)] complex on mesoporous silica nanoparticles (1×10^{-5} M)⁴⁵. In addition, The peroxidase activity of Cu NPs with that of gold nanoparticles has been compared (Table S1 and S2). For nature enzymes, K_m indicates the affinity for the substrate. So, a smaller K_m means higher affinity. The K_m value

for the Cu NPs was 1.047 mM, which is much lower than that of the AuNPs/PVP-GNs (2.63 mM). The result indicated that the Cu NPs prepared in our experiment have a significantly higher affinity than AuNPs/PVP-GNs.

3.5 Determination of glucose in the pear juice and blood samples

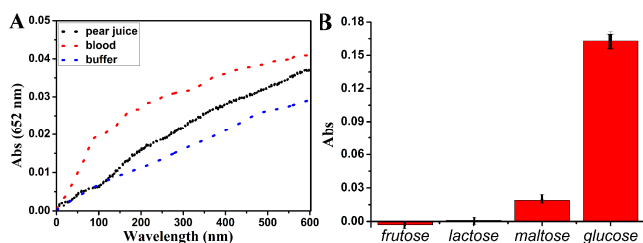


Fig. 5 (A) Time-dependent absorbance changes at 652 nm for different samples (buffer solution, diluted blood and pear juice samples) after incubation with GOx. Blood and pear juice was diluted 500-fold, respectively. (B) Selectivity analysis for glucose detection by monitoring the relative absorbance. The analyte concentrations were as follows: 10 mM fructose, 10 mM lactose, 10 mM maltose, and 5 mM glucose. The error bars represent the standard deviation of three measurements.

In order to test the selectivity of the colorimetric method for glucose, 10 mM fructose, 10 mM lactose, and 10 mM maltose were used as control samples, respectively. Fig. 5B shows the absorbance of solution in the presence of glucose or other analogues. The obvious difference of solution absorbance can be observed between glucose and the analogues, even the concentration of analogues were 2 times higher than that of glucose. The main reason is that glucose oxidase has a certain degree of specificity to oxidized glucose, so the absorbance hardly increased for glucose, fructose, lactose and maltose in Fig. 5B. Even though the control sample was used at the concentrations of 10 mM, the signal remained as low as the background signal. On this basis, we developed a simple, speed, and highly selective and sensitive colorimetric method to detect glucose. To test the application of this method on real samples, blood sample and pear juice were used to determine their glucose concentration. Fig. 5A shows the time-dependent absorbance changes of solutions in the absence or presence of samples. The concentrations of glucose in blood and pear juice were 59.7 μ M and 49.4 μ M, respectively. Therefore, glucose would be detected by colorimetric method in medical diagnostic and biological analysis.

4. Conclusions

In summary, stable Cu NPs were prepared by a facile method using humic acid as a stabilizing and reducing agent. Cu NPs can generate a blue color reaction in the presence of H₂O₂ and TMB. Additionally, the prepared Cu NPs were very stable in a long period time of six months. Furthermore, utilizing the Cu NPs as a biosensor platform, H₂O₂ and glucose can be detected ranging from 1.5×10^{-7} to 1.25×10^{-5} M and 1×10^{-6} to 1×10^{-4} M respectively. On this basis, we promote a novel simple ultrasensitive and highly selective colorimetric strategy to detect glucose in blood and pear juice samples. The prepared stable Cu NPs with high catalytic activity is valuable, which would have potential application in medical diagnostics and biotechnology.

Acknowledgements

This work was supported by the National Natural Science Foundation of China (No. 21375079, No. 51402175) and Project of Development of Science and Technology of Shandong Province, China (No. 2013GZX20109).

Notes and references

Corresponding author: College of Chemistry and Material Science, Shandong Agricultural University, Taian, 271018, P. R. China

Tel: +86 538 8247660

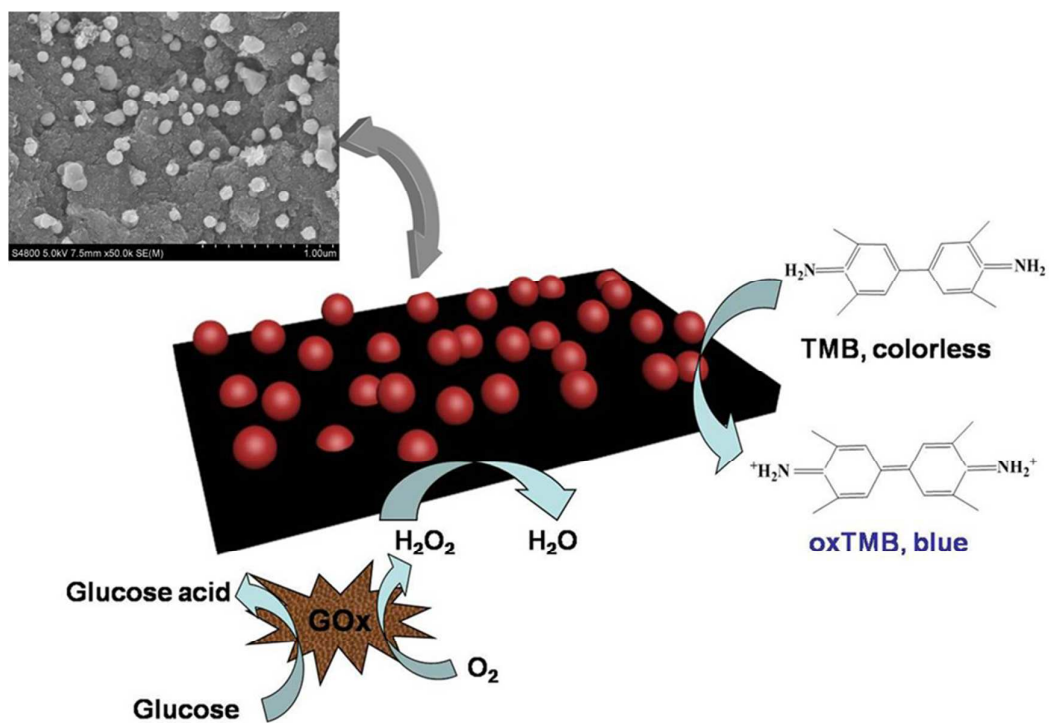
Fax: +86 538 8242251

E-mail address: fanhai@sdau.edu.cn
ashy@sdau.edu.cn

1. W. B. Kannel and D. McGee, *Diabetes care*, 1979, **2**, 120-126.
2. M. Tominaga, H. Eguchi, H. Manaka, K. Igarashi, T. Kato and A. Sekikawa, *Diabetes care*, 1999, **22**, 920-924.
3. R. F. Irvine, *Biochem. J.*, 1982, **204**, 3, 295-305.
4. H.-P. Hersleth, U. Ryde, P. Rydberg, C. H. Görbitz and K. K. Andersson, *J. Inorg. Biochem.*, 2006, **100**, 460-476.
5. M. Hamid, *Food Chem.*, 2009, **115**, 1177-1186.
6. H. Wei and E. Wang, *Anal. Chem.*, 2008, **80**, 2250-2254.
7. Y. Lu and W. Chen, *Chem. Soc. Rev.*, 2012, **41**, 3594-3623.
8. L. Shang, S. Dong and G. U. Nienhaus, *Nano Today*, 2011, **6**, 401-418.
9. H. Xu and K. S. Suslick, *ACS Nano*, 2010, **4**, 3209-3214.
10. M. Ma, Y. Zhang and N. Gu, *Colloids Surf. A*, 2011, **373**, 6-10.
11. Y. Jv, B. Li and R. Cao, *Chem. Commun.*, 2010, **46**, 8017-8019.
12. Y. Zhang, C. Xu, B. Li and Y. Li, *Biosens. Bioelectron.*, 2013, **43**, 205-210.
13. X.-X. Wang, Q. Wu, Z. Shan and Q.-M. Huang, *Biosens. Bioelectron.*, 2011, **26**, 3614-3619.
14. Y. Tao, Y. Lin, J. Ren and X. Qu, *Biosens. Bioelectron.*, 2013, **42**, 41-46.
15. X. Xia, Y. Zhang and J. Wang, *RSC Adv.*, 2014, **4**, 25365-25368.
16. L. Chen, N. Wang, X. Wang and S. Ai, *Microchim. Acta*, 2013, **180**, 1517-1522.
17. C. Hu, D.-P. Yang, F. Zhu, F. Jiang, S. Shen and J. Zhang, *ACS Appl. Mater. Interfaces*, 2014, **6**, 4170-4178.
18. Y. Chen, H. Cao, W. Shi, H. Liu and Y. Huang, *Chem. Commun.*, 2013, **49**, 5013-5015.
19. H. Chen, Y. Li, F. Zhang, G. Zhang and X. Fan, *J. Mater. Chem.*, 2011, **21**, 17658-17661.
20. C.-W. Tseng, H.-Y. Chang, J.-Y. Chang and C.-C. Huang, *Nanoscale*, 2012, **4**, 6823-6830.
21. Y. Guo, L. Deng, J. Li, S. Guo, E. Wang and S. Dong, *ACS Nano*, 2011, **5**, 1282-1290.
22. C.-W. Lien, C.-C. Huang and H.-T. Chang, *Chem. Commun.*, 2012, **48**, 7952-7954.
23. A. C. Jones, R. L. Olmon, S. E. Skrabalak, B. J. Wiley, Y. N. Xia and M. B. Raschke, *Nano Lett.*, 2009, **9**, 2553-2558.
24. S. B. Kalidindi and B. R. Jagirdar, *ChemSusChem*, 2012, **5**, 65-75.
25. N. Tian, Z.-Y. Zhou, S.-G. Sun, Y. Ding and Z. L. Wang, *science*, 2007, **316**, 732-735.
26. H. Bai, M. Han, Y. Du, J. Bao and Z. Dai, *Chem. Commun.*, 2010, **46**, 1739-1741.
27. S. Guo and E. Wang, *Nano Today*, 2011, **6**, 240-264.
28. H. Cao, Z. Chen, H. Zheng and Y. Huang, *Biosens. Bioelectron.*, 2014, **62**, 189-195.
29. Y. Zhong, J. Zhu, Q. Wang, Y. He, Y. Ge and C. Song, *Microchim. Acta*, 2015, **182**, 909-915.
30. R. R. Arvizo, S. Bhattacharyya, R. A. Kudgus, K. Giri, R. Bhattacharya and P. Mukherjee, *Chem. Soc. Rev.*, 2012, **41**, 2943-2970.
31. A. Quarta, R. Di Corato, L. Manna, S. Argentiere, R. Cingolani, G. Barbarella and T. Pellegrino, *J. Am. Chem. Soc.*, 2008, **130**, 10545-10555.
32. M. Jin, G. He, H. Zhang, J. Zeng, Z. Xie and Y. Xia, *Angew. Chem. Int. Ed.*, 2011, **50**, 10560-10564.

33. D. Zhang, R. Wang, M. Wen, D. Weng, X. Cui, J. Sun, H. Li and Y. Lu, *J. Am. Chem. Soc.*, 2012, **134**, 14283-14286.
34. Y. Song, K. Qu, C. Zhao, J. Ren and X. Qu, *Adv. Mater.*, 2010, **22**, 2206-2210.
35. Y. Chang, M. L. Lye and H. C. Zeng, *Langmuir*, 2005, **21**, 3746-3748.
36. D. Mott, J. Galkowski, L. Wang, J. Luo and C.-J. Zhong, *Langmuir*, 2007, **23**, 5740-5745.
37. Y. Wei, S. Chen, B. Kowalczyk, S. Huda, T. P. Gray and B. A. Grzybowski, *J. Phys. Chem. C*, 2010, **114**, 15612-15616.
38. M. Jin, G. He, H. Zhang, J. Zeng, Z. Xie and Y. Xia, *Angew. Chem. Int. Ed.*, 2011, **50**, 10560-10564.
39. M. Guerrero, S. Pané, B. J. Nelson, M. D. Baró, M. Roldán, J. Sort and E. Pellicer, *Nanoscale*, 2013, **5**, 12542-12550.
40. L. Hu, Y. Yuan, L. Zhang, J. Zhao, S. Majeed and G. Xu, *Anal. Chim. Acta*, 2013, **762**, 83-86.
41. L. Chen, B. Sun, X. Wang, F. Qiao and S. Ai, *J. Mater. Chem. B*, 2013, **1**, 2268-2274.
42. M. Liu, H. Zhao, S. Chen, H. Yu and X. Quan, *ACS Nano*, 2012, **6**, 3142-3151.
43. L. Chen, K. Sun, P. Li, X. Fan, J. Sun and S. Ai, *Nanoscale*, 2013, **5**, 10982-10988.
44. P. Mondal, A. Sinha, N. Salam, A. S. Roy, N. R. Jana and S. Islam, *RSC Adv.*, 2013, **3**, 5615-5623.
45. S. SenáGupta, *Chem. Commun.*, 2012, **48**, 5289-5291.

Graphical Abstract



Stable Cu NPs were prepared using humic acid as the reducing and stabilizing agent for application in glucose detection.